Macromolecules
ARTICLE

*Macromolecules* **2010**, *43*, 7321–7329 **7321**
DOI: 10.1021/ma101349t

# Two-Dimensional Size/Branch Length Distributions of a Branched Polymer

**Francisco Vilaplana and Robert G. Gilbert***

*The University of Queensland, Centre for Nutrition and Food Sciences and School of Land, Crop and Food Sciences, Hartley Teakle Building, Brisbane, Queensland 4072, Australia*

*Received June 18, 2010*

ABSTRACT: The first two-dimensional structural distributions are reported for a hyperbranched polymer, the two dimensions being macromolecular size and individual branch length. The 2D distributions for native starch, a polymer with both short- and long-chain branched components (amylopectin and amylose), were obtained by size fractionation using size-exclusion chromatography combined with enzymatic debranching. These distributions show distinct macromolecular architectures: separate "mountains" corresponding to amylopectin and amylose and two "foothills" assigned to hybrid populations. The distributions reveal new mechanistic information on the underlying polymer synthesis. The branch-length distributions for amylopectin are independent of macromolecular size, whereas a size variation is observed for amylose. Biological imperatives in amylopectin biosynthesis force the same branching structure for all macromolecular sizes because of evolutionary pressure to provide the crystallinity indispensable for the plant survival. Amylose biosynthesis does not have such restrictive biological constraints, offering a range of branched structures throughout macromolecular sizes and revealing a previously unsuspected size dependence.

## Introduction

Size separation of polymers (e.g., using size-exclusion chromatography or field-flow fractionation) separates by hydrodynamic volume $V_h$ (the definition of which[1] depends on the technique employed). For linear (homo)polymers, there is a one-to-one relationship between the molecular weight $M$ and $V_h$; thus (in principle), complete structural information for a linear (atactic) homopolymer can be obtained from a one-dimensional distribution, using size separation together with a single mass- or number-sensitive detector (although another detector may sometimes be required to find the relation between $M$ and $V_h$). This one-to-one relationship does not hold for complex branched polymers, and indeed an infinite-dimensional distribution is required to completely specify the distribution of structures of a sample of a branched homopolymer.[2] One-dimensional separation techniques with different detectors characterize different one-dimensional projections of the structural distribution: e.g., number, total weight, and weight-average molecular weight size distributions from viscometric, differential refractive index (DRI), and multiple-angle laser light scattering (MALLS) detectors, respectively. While such one-dimensional projections provide useful information, it is clear that new information sensitive both to the underlying synthetic processes and to structure−property relations could be obtained with two-dimensional distributions. No fully characterized 2D technique has yet been reported for the simultaneous analysis of branched polymers based on size and branching structure. Comprehensive 2D liquid chromatography, combining SEC and interaction chromatography, enables the separation and further structural analysis of complex (co)polymers based on size and chemical composition (e.g., refs 3−5), but these setups may not be applicable for the characterization of branched polymers with complex architectures. Molecular-topology fractionation is an elegant method which has been successfully implemented to separate by both branching structure and $V_h$,[6,7] but a problem is that the branching separation parameter has not been worked out for this technique (although methods are emerging to do this[8]).

In this paper, the first full 2D structural distribution of a branched homopolymer is reported, where the two structural dimensions are total size of a molecule ($V_h$) and the degree of polymerization (DP) of a branch in that molecule. This experimental distribution is found for starch, taking advantage of the fact that all branches in this polymer can be quantitatively cut using a debranching enzyme; the method can also be applied to synthetic branched polymers where quantitative debranching is possible (e.g., ref 9). The application of this new technique to native starch will be seen to shed new light on the mechanisms involved in its biosynthesis.

Starch is a homopolymer of anhydroglucose, where the α-D-glucopyranosyl monomeric units are lineally extended by (1→4) linkages and branches are formed by (1→6) bonds at the branching points. Starch comprises basically two types of macromolecular branch structure: amylose, with relatively low molecular weight ($10^5$−$10^6$ Da) and a few long-chain branches, and amylopectin, with much higher molecular weight ($10^7$−$10^9$ Da) and hyperbranched, having an enormous number of very-short-chain branches. Using a polymer with distinct both short- and long-chain branching components is useful for distinguishing effects that can arise from these different branching architectures. Starch also has a higher level of structure: neighboring amylopectin branch clusters in (undissolved and ungelatinized) native starch form α-helices, resulting in alternating crystalline and amorphous lamellae (these lamellae themselves form higher structural levels). Shorter amylopectin branches are confined to a single crystalline lamella, while a few longer amylopectin branches span two or more lamellae. Both amylose and amylopectin have a broad distribution of sizes and molecular weights, which depend on plant variety.

The method used here to obtain 2D distributions uses preparative size-exclusion chromatography and enzymatic debranching;[2] pioneering work by Ball and co-workers[10,11] and by Jane and co-workers[12] also used this combination of techniques, but systematic 2D structural distributions were not reported. Preparative SEC is

*Corresponding author: Tel +61 7 3365 4809; Fax +61 7 3365 1188; e-mail b.gilbert@uq.edu.au.

© 2010 American Chemical Society

Published on Web 08/06/2010

used here to yield starch fractions having different average hydrodynamic volumes; the weight distributions of the size-separated fractions are individually characterized using analytical SEC. These individual fractions are then enzymatically debranched, and the resulting samples of linear polysaccharides also characterized using analytical SEC. The result is a two-dimensional distribution: the weight of branched starch molecules having a given $V_h$ and (after debranching) a branch with a given DP $X_{de}$. The information from this distribution, being for a sample of essentially undegraded native starch (from rice), will be seen to enable a number of qualitative inferences to be made about starch biosynthesis. The methodology used here has considerable potential to be used in the future for quantitative information on (bio)synthesis and structure−property relations for starch and for those synthetic polymers where quantitative debranching is possible.

## Experimental Section

**Materials and Sample Preparation.** Native rice starch flour (MRQ74) from MARDI (Kuala Lumpur, Malaysia), with a total starch content of 84.28 ± 0.23% as measured using the Total Starch Kit (Megazyme, Wicklow, Ireland) and a amylose content in starch of 27% (reported by the supplier), was extracted from the whole rice grain using dimethyl sulfoxide (DMSO). Starch samples for chromatographic fractionation and analysis were prepared by dissolving directly in the SEC eluent, consisting of DMSO (ACS grade, Merck) with 0.5% w/w LiBr (ReagentPlus) for 8 h without stirring in a thermomixer set at 80 °C. The concentrations were fixed at 10 g $L^{-1}$ for preparative SEC and 2 g $L^{-1}$ for analytical SEC. This procedure has been reported to completely dissolve starch while also minimizing degradation during sample preparation.[13]

**Fractionation of Starch by Size Using Preparative SEC.** Rice starch was fractionated with a PREP GRAM precolumn, a PREP GRAM 30, and PREP GRAM 3000 columns from PSS (Mainz, Germany) in a AF2000 setup (Postnova Analytics, Landsberg-Lech, Germany), kept at 80 °C, with a mobile phase flow rate of 1.5 mL $min^{-1}$ DMSO/LiBr 0.5%. Sample volumes of 1 mL with concentrations of 10 g $L^{-1}$ were manually injected using a Rheodyne 7000 high-pressure switching valve (IDEX Health & Science LLC, Rohnert Park, CA). Ten fractions were collected manually at different elution volumes (and were therefore fractionated by hydrodynamic volume). Each fraction was then further analyzed separately to obtain the size distribution of the branched molecules (first dimension) and, following debranching, the chain-length distribution (CLD) of the branches (second dimension).

Using SEC for finding the CLD of the short branches of amylopectin is not without problems because SEC suffers from significant band broadening in this range.[14] While fluorophore-assisted capillary electrophoresis[15,16] (FACE) does not suffer from these problems for (linear) starch oligomers, this technique is currently constrained to relatively low DPs (≲80) and thus cannot be used for the amylose component of starch; SEC is currently the best separation method for larger oligomers. As one objective in the present study is to look at any systematic differences between the 2D distributions of these two starch components, SEC was used to cover the whole range of the second dimension (branch length).

**Size Analysis of the Whole (Branched) Molecules.** An aliquot of each collected fraction was taken, precipitated overnight by adding 5:1 v/v in proportion of absolute ethanol (grade for analysis, Merck) (ethanol:DMSO), and centrifuged at 4000 rpm in an Allegra X-13 R centrifuge (Beckman Coulter, Brea, CA). The supernatant was discarded, and the remaining starch precipitates were redissolved in SEC eluent prior to analysis. The size distributions of the branched fractions were obtained using an Agilent 1100 series system (PSS, Mainz, Germany) equipped with a GRAM precolumn and 30 and 3000 analytical columns (PSS). 100 μL samples were injected in the SEC system with DMSO/LiBr 0.5% w/w as the mobile phase at a flow rate of 0.3 mL $min^{-1}$ and 80 °C. Triple detection was performed by a setup consisting of multiple-angle laser light scattering (MALLS; BIC-$M_w$A7000, Brookhaven Instrument Corp., New York), followed by parallel flow into a refractive index detector (RID; Shimadzu RID-10A, Shimadzu Corp., Japan) and a viscometric detector (ETA-2010, PSS).

**Debranching of Starch Fractions and Size Analysis of the Branches.** The remaining sample from each preparative fraction was precipitated and centrifuged using the same procedure as for the branched fractions and debranched as follows with isoamylase from *Pseudomonas sp.* (Megazyme, Wicklow, Ireland). The starch fractions were dispersed with 9 mL of deionized water and heated in a boiling water bath for 15 min with gentle stirring. The dispersion was cooled to room temperature and incubated in a water batch at 37 °C for 4 h after adding 20 μL of sodium azide solution in deionized water (0.1 g $mL^{-1}$), 1 mL of 0.1 M sodium acetate buffer (pH 3.5), and 5 μL of the enzyme solution. The enzyme was deactivated by immersion of the solution in boiling water for 15 min. The debranched fractions were immediately frozen, to avoid retrogradation of the debranched chains, until subsequent freeze-drying in a VirTis Benchtop K freeze-dryer (VirTis, Gardiner, NY), and finally redissolved in DMSO/LiBr 0.5% w/w prior to SEC analysis.

The branch size distributions were analyzed using the same SEC setup described for branched molecules, with triple detection. Separation of the debranched fractions was performed in this case with combined GRAM precolumn 100 and 1000 analytical columns (PSS) with a flow rate of 0.6 mL $min^{-1}$ DMSO/LiBr 0.5% w/w at 80 °C.

**SEC calibration** was performed using pullulan standards with molecular weights ranging from 342 to 1.66 × $10^6$ Da (PSS, Mainz, Germany). The standards were dissolved in the SEC eluent and injected into the branched and debranched SEC setups to provide universal calibration curves to relate elution volume $V_{el}$ with $V_h$. The Mark−Houwink parameters for pullulan in DMSO/LiBr (0.5 wt %) at 80 °C are $K = 2.427 \times 10^{-4}$ dL $g^{-1}$ and $a = 0.6804$, while the $dn/dc$ value is 0.0853 mL $g^{-1}$ (Kramer and Kilz, PSS, Mainz, private communication).

**Data Processing and Size Distributions from Sec Coupled with Multiple Detection.** The data recorded after the analytical SEC separations and multiple detection were processed using WinGPC software (PSS) and further analyzed by additional procedures to obtain different size distributions.[2,17] For branched starch, the results from SEC are presented for sake of clarity in terms of hydrodynamic radius ($R_h$), with $V_h = {}^4/_3\pi R_h^3$. DRI detection provides the so-called SEC weight distribution $w(\log V_h)$ through eq 1, and the number distribution $N(V_h)$ is derived from the specific viscosity ($\eta_{sp}$), directly obtained from the viscometric detector (eq 2).[2]

$$w(\log V_h) = -S_{DRI}(V_{el})\frac{d\tilde{V}_{el}(V_h)}{d \log V_h} \quad (1)$$

$$N(V_h) = -\frac{\eta_{sp}(V_{el})}{{V_h}^2}\frac{d\tilde{V}_{el}(V_h)}{d \log V_h} \quad (2)$$

Here $S_{DRI}(V_{el})$ is the DRI signal, $\eta_{sp}$ is the specific viscosity obtained from the viscometric detector, and $\tilde{V}_{el}(V_h)$ is the universal calibration curve giving the dependence of elution volume on hydrodynamic volume.

Throughout this paper, the (overall) weight-average molecular weight for the unseparated sample is denoted $\bar{M}_w$, while the average molecular weight in an increment of hydrodynamic volume is denoted $\bar{M}_w(V_h)$ (and similarly for the radius of gyration). The size dependences of the weight-average molecular weight, $\bar{M}_w(V_h)$, and of the root-mean-square weight-average radius of gyration, $\bar{R}_g(V_h)$, are obtained from the MALLS and the DRI signals, using the differential refractive index ($dn/dc$) for the macromolecule in the solvent system at the temperature of the detector. The value of $dn/dc = 0.0544$ mL $g^{-1}$ for rice starch in DMSO/LiBr 0.5% w/w at 80 °C (measured by PSS, Mainz) was employed for the branched rice starch calculations;

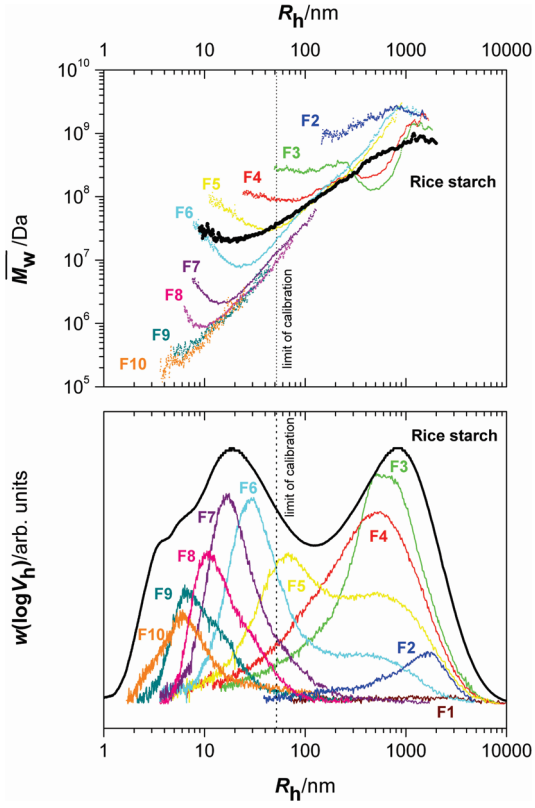


**Figure 1.** SEC weight [$w(\log V_h)$] and weight-average molecular weight [$\bar{M}_w(V_h)$] distributions for the rice starch fractions, as functions of the hydrodynamic radius of these branched samples. Broken vertical line: upper limit of SEC calibration. F2−F10 denote fractions collected in the preparative SEC, with average sizes of the full (undebranched) fractions decreasing from F2 to F10 (Table 1). The thick black line denoted "rice starch" is the parent (unfractionated) sample.

for the case of debranched linear rice starch molecules, d$n$/d$c$ was taken to be 0.0689 mL g$^{-1}$ (measured by PSS, Mainz, for amylose in the solvent and temperature of this study).

## Results

**Fractionation of Rice Starch and Size Distributions of the Branched Fractions.** Size fractionation of rice starch was performed using preparative SEC, as detailed in the Supporting Information. These size-separated fractions were further characterized using analytical SEC to give the size distributions of these fractions. If separation were perfect, these would be perfectly monodisperse in size, but in actuality one sees distributions of moderate width, the average of which increases with decreasing elution time for the preparative SEC (band broadening is worse in preparative SEC than in analytical SEC). $\bar{M}_w(V_h)$ and $w(\log V_h)$ for the whole rice starch sample and its fractions are given in Figure 1. The SEC distributions of the different fractions progress within the envelope of the original distribution of the parent (unfractionated) rice starch sample. The $\bar{M}_w(V_h)$ distributions of the consecutive fractions also tend to lower molecular-weight values with smaller size. For example, fractions F5 and F6 display a well-defined two-peak size distribution in the analytical SEC runs, corresponding to amylopectin and amylose.

SEC of extremely large molecules such as amylopectin suffers both from calibration problems with standards and from shear scission of the biggest molecules.[18] Indeed, the $\bar{M}_w(V_h)$ distributions for the amylopectin-rich fractions (F3 and F4) show anomalous shapes precisely in the region that is beyond the calibration range, which can be attributed to the poor separation of amylopectin molecules using SEC. These technical limitations of the SEC fractionation and collection procedure do not affect inferences that will be made from the experimental data (other size separation techniques such as flow field-flow fractionation may reduce shear scission,[19,20] but as yet no reliable data for undegraded native starch using any variant of this technique have appeared in the literature). The lower size fractions F9 and F10 probably include some impurities from proteins and lipids retained in the rice flour (Supporting Information).[21]

**Table 1. Properties of the Branched Molecules in the Collected Fractions**[a]

| sample | fractionation volumes $(V_{el})_{PREP}$ (mL) | log($\bar{R}_h$/nm) | $\bar{M}_w$ (Da) | $\bar{R}_g$ (nm) |
|---|---|---|---|---|
| rice starch | | 1.35 | $2.08 \times 10^8$ | 222 |
| F1 | 58.00−62.35 | 3.34 | $3.11 \times 10^8$ | 354 |
| F2 | 62.35−65.25 | 3.04 | $4.44 \times 10^9$ | 538 |
| F3 | 65.25−69.60 | 2.82 | $2.81 \times 10^8$ | 254 |
| F4 | 69.60−73.95 | 2.56 | $3.45 \times 10^8$ | 245 |
| F5 | 73.95−79.75 | 2.06 | $5.09 \times 10^8$ | 251 |
| F6 | 79.75−85.55 | 1.65 | $1.58 \times 10^8$ | 190 |
| F7 | 85.55−91.35 | 1.17 | $6.11 \times 10^6$ | 91 |
| F8 | 91.35−97.15 | 1.10 | $2.99 \times 10^6$ | |
| F9 | 97.15−104.40 | 0.89 | $1.96 \times 10^6$ | |
| F10 | 104.40−113.10 | 0.67 | $3.72 \times 10^5$ | |

[a] Average macromolecular size log($\bar{R}_h$); average weight-average molecular weight, $\bar{M}_w$; and root-mean-square weight-average radius of gyration, $\bar{R}_g$.

The average size and molecular weight values for the different branched fractions are given in Table 1. The average hydrodynamic radius of the branched macromolecules, log($\bar{R}_h$), is obtained using an equivalent expression to the number-average molecular weight for linear polymers, defined here by eq 3:

$$\log(\bar{R}_h) = \frac{\int_{-\infty}^{\infty} w(\log V_h)\, \mathrm{d} \log R_h}{\int_{-\infty}^{\infty} \dfrac{w(\log V_h)}{\log R_h}\, \mathrm{d} \log R_h} \qquad (3)$$

This average hydrodynamic radius decreases progressively for the different collected fractions. The $\bar{M}_w$ values decrease for consecutive fractions, with some deviations for the amylopectin-rich fractions that is attributed to band broadening. These values, in the range of $10^7-10^8$ and $10^5-10^6$ Da for the amylopectin-rich and amylose-rich fractions, respectively, are in agreement with previous studies for rice starch.[22] The overall radius of gyration $\bar{R}_g$ results for the different fractions follow similar behavior, with values ranging between 200 and 550 nm for the amylopectin-rich fractions. $\bar{R}_g$ values could not be obtained with precision for the different amylose-rich fractions (F7 to F10) using MALLS; this could be due to the low concentrations and sizes of the amylose macromolecules in the sample and to interference from amylopectin populations present in these fractions that biased the results to higher (and unrealistic) $\bar{R}_g$ values (MALLS is sensitive to higher molecular weights and works best with higher concentrations).

**Debranched Chain-Length Distributions.** The enzymatically debranched starch fractions were analyzed using the analytical SEC setup with multiple detection. Figures 2 and 3 show the comparative of the branched and debranched distributions for the whole (unfractionated) rice starch sample and the different fractions, respectively. The branched and debranched $w(\log V_h)$ and $N(V_h)$ distributions for the parent unfractionated rice starch (Figure 2) show the usual characteristic features. Two clear peaks at $R_h \sim 10^3$ and ~30 nm are observed in the branched distributions, corresponding to amylopectin and amylose,

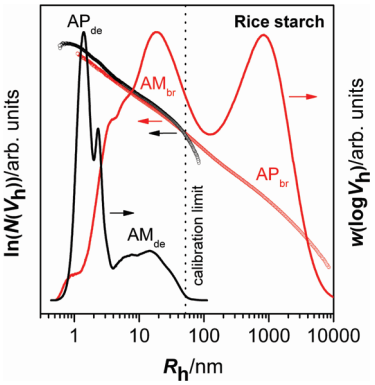


**Figure 2.** Comparison of the SEC weight $w(\log V_h)$ and number $N(V_h)$ distributions for the branched (red points) and debranched (black points) for the parent (unfractionated) rice starch. Broken vertical line: upper limit of SEC calibration. AM = amylose, AP = amylopectin, br = branched, de = debranched.

respectively; the debranched distributions show a bimodal peak for the short amylopectin branches (at $R_h \sim 1.5$ nm) and another bimodal peak for the amylose branches at $R_h \sim 20$ nm, a behavior typical of such distributions found in the literature. Figure 3 gives the $N(V_h)$ of branched and debranched distributions for the collected fractions. The branched and debranched $N(V_h)$ in the amylopectin-rich (largest branched size) fractions (F1 to F4) are distinctly different, as expected; the smaller fractions F5 and F6 show features of both amylose and amylopectin populations, and the smallest fractions (F7−F10) show that the branched and debranched distributions for the amylose chains are similar.

The debranched size distributions, being for linear chains, can be expressed in terms of either hydrodynamic volume, or in terms of (debranched) molecular weight, or in terms of (debranched) DP. Because of band broadening in the SEC separation of the debranched samples, this last has to be in terms of an average (debranched) degree of polymerization, $\bar{X}_{de}$. This is obtained using MALLS and DRI detection; thus, $\bar{X}_{de}$ is a weight average. A master calibration curve (Supporting Information) to convert elution volume ($\tilde{V}_{el}$) into $\bar{X}_{de}$ was obtained using the data from the different fractions. (In practice, only the amylose-rich fractions provided a sufficient MALLS signal for this procedure, due to the small molar mass of the amylopectin linear branches.) The debranched SEC weight distributions were then obtained from the DRI signal in the usual way; for linear polymers, $w(\log \bar{X}_{de})$ and $N(\bar{X}_{de})$ are related by eq 4 (e.g., refs 23 and 24):

$$w(\log \bar{X}_{de}) = \bar{X}_{de}^{\,2} N(\bar{X}_{de}) \qquad (4)$$

The resulting distributions are plotted in Figure 4 for the whole rice starch sample and the preparative fractions. These fraction distributions together constitute the desired 2D distribution, plotted in Figure 5. The debranched distributions display distinct populations corresponding to short amylopectin ($\bar{X}_{de} \sim 5-125$) and longer amylose ($\bar{X}_{de} \sim 400-20\,000$) branches. The debranched distributions have the features familiar in the starch literature, which for convenience here are discussed in terms of three regions: zone AP1 ($\bar{X}_{de} \sim 5-30$) corresponding to the short (single-lamella) branches of amylopectin; zone AP2 ($\bar{X}_{de} \sim 40-125$), corresponding to the slightly longer, lamella-spanning, chains of amylopectin; and AM3 ($\bar{X}_{de} \sim 400-20\,000$), corresponding to the amylose branches. (The amylose debranched distribution in this zone may be bi- or trimodal, as seen in the many literature examples of debranched distributions of unfractionated amylose.)

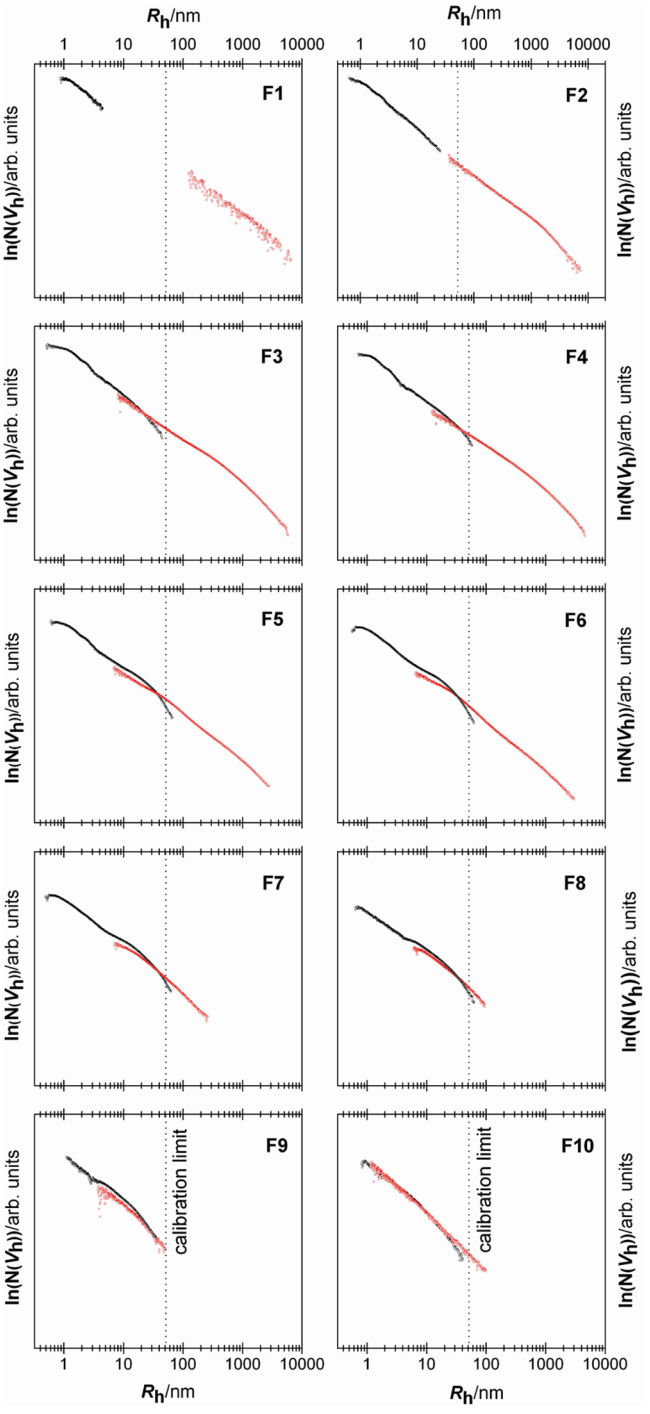


**Figure 3.** Comparison of the number distributions $N(V_h)$ for the branched (red points) and debranched (black points) for the starch fractions, with average sizes of the full (undebranched) fractions decreasing from F2 to F10. Broken vertical line: upper limit of SEC calibration.

Interestingly, the amylopectin-type short branch distributions in regions AP1 and AP2 can be observed in all the collected fractions, even for the smaller macromolecular sizes corresponding to amylose regions. When renormalized to all have the same maximum in AP1, the quantitative forms of $w(\log \bar{X}_{de})$, and hence also of $N(\bar{X}_{de})$, for the amylopectin debranched zones AP1 and AP2 are essentially the same for all the collected fractions. This indicates that the branch chain-length distributions for amylopectin are not influenced by their macromolecular size. On the other hand, the branch chain-length distribution for the amylose region

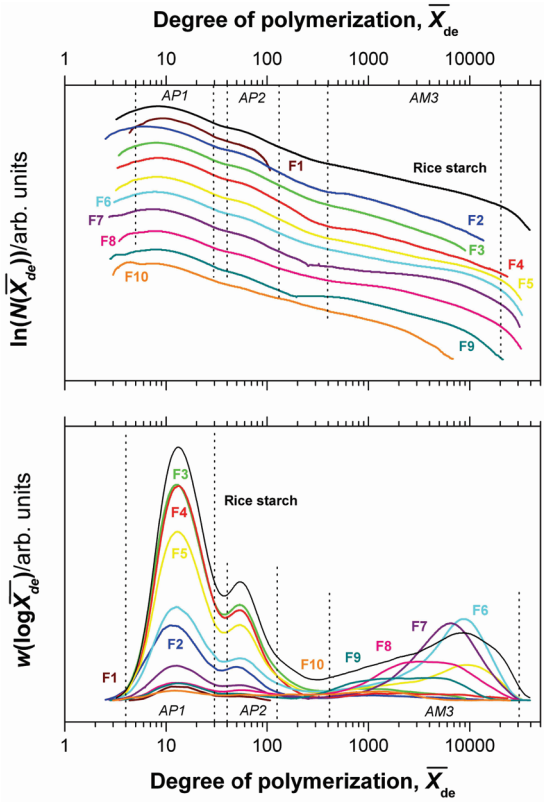


**Figure 4.** SEC weight [$w(\log \bar{X}_{de})$] and number [$N(\bar{X}_{de})$] distributions for debranched rice starch and the fractions as functions of degree of polymerization. Three zones in the debranched distributions can be observed: AP1 and AP2, the short branches of amylopectin, and AM3, the long branches of amylose.

AM3 exhibits significant variations for the different fractions. For the amylopectin-rich fractions F2−F4, a small peak appears in the $w(\log \bar{X}_{de})$ distributions at $\bar{X}_{de} \sim 1000$, which indicates the presence of medium-sized branches that do not correspond with the typical short branches for the amylopectin populations. The implications of this macromolecular architecture for understanding the biosynthetic pathway for rice starch will be discussed in the following section.

Results for the number- and weight-average debranched DPs, $\bar{X}_{de,n}$ and $\bar{X}_{de,w}$, are presented in Table 2. As expected from the shape of the SEC weight distributions, the values of these quantities for the amylopectin regions AP1 and AP2 do not systematically vary for the different fractions and are in a similar range to those reported by many authors for various rice starch varieties (e.g., refs 25−27). On the other hand, $\bar{X}_{de,n}$ and $\bar{X}_{de,w}$ for the amylose region AM3 decrease systematically with decreasing branched macromolecular size. The values of $\bar{X}_{de,n}$ and $\bar{X}_{de,w}$ for the amylose region given here are slightly higher than those reported using wet chemistry and SEC with fluorescent labeling[28,29] and similar to those obtained by SEC and light scattering.[30]

**Two-Dimensional Size/Branch Chain-Length Distributions.** The two-dimensional size distributions, based on macromolecular size $\bar{R}_h$ as the first dimension and chain-length distribution of the branches $\bar{X}_{de}$ as the second dimension, were obtained from the experimental branched and debranched distributions of the collected fractions from preparative SEC, using the Renka−Cline random-gridding method implemented by Origin 7.0 software. The plots of the 2-dimensional SEC weight $w(\log(\bar{R}_h,\bar{X}_{de}))$ and number $N(\bar{R}_h,\bar{X}_{de}))$ distributions are presented in Figures 5a and 5b,

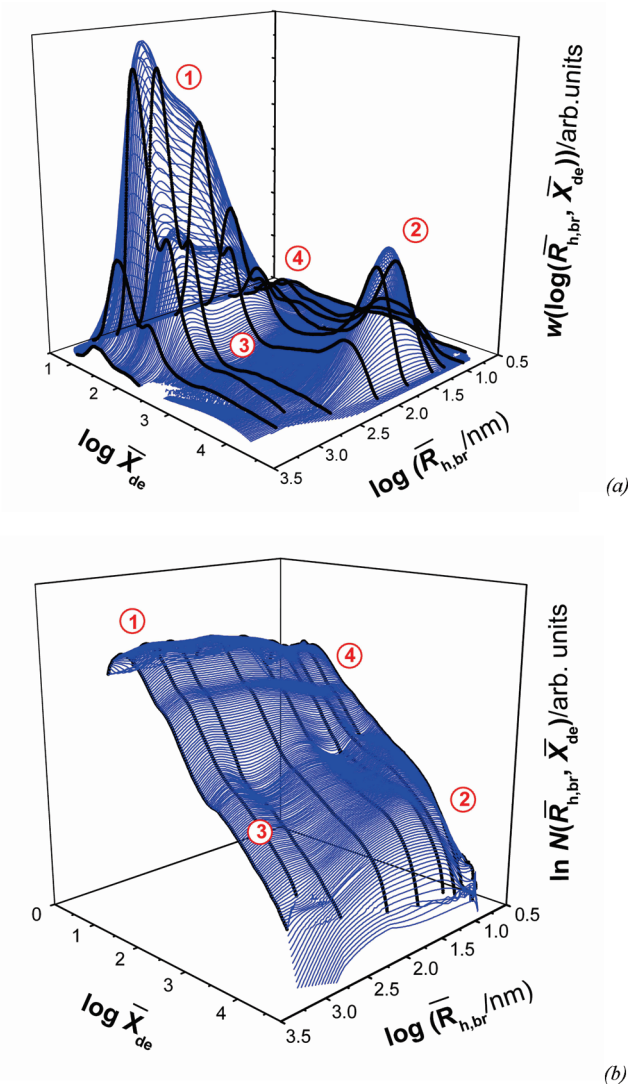


**Figure 5.** Two-dimensional experimental distributions for rice starch based on macromolecular size and branch chain length: (a) SEC weight distribution $w(\log(\bar{R}_h,\bar{X}_{de}))$; (b) number distribution $N(\bar{R}_h,\bar{X}_{de})$; the size axis is labeled $\bar{R}_{h,br}$ to emphasize that this refers to the fully branched (whole) molecule. The black points correspond to the experimental data from each collected fraction from preparative SEC. The blue surfaces correspond to the mathematical distributions after Renka−Cline random gridding. The four features (two "mountains" and two "foothills") described in the text are indicated.

respectively. As discussed later, there are four features (maxima), two "mountains" and two "foothills", in these distributions.

**Kinetic Analysis of the Chain-Length Distribution of the Debranched Starch Fractions.** As well as the maxima of the four features seen in Figure 5, information can be obtained from other details of the distribution. This requires some model of starch biosynthesis, which is an extremely complex process involving interconnected phenomena that occur simultaneously in the plant endosperm. A simplified treatment based on general kinetic principles[31] suggests that the debranched distribution can be plotted as $\ln N(\bar{X}_{de})$ against $\bar{X}_{de}$, when straight-line regions give an indication of the relative rates of chain growth and chain stoppage. A more advanced treatment[2] which takes specific account of the mechanisms of the enzymes catalyzing branching, debranching, and propagation (starch branching enzymes, starch debranching enzymes, and starch synthase, respectively)

**Table 2. Properties of the Debranched Molecules in the Collected Fractions for the Three Regions in the Chain-Length Distributions[a]**

| | | zone AP1 ($\bar{X}_{de} \sim 5-30$) | | zone AP2 ($\bar{X}_{de} \sim 40-125$) | | zone AM3 ($\bar{X}_{de} \sim 400-20000$) | | |
|---|---|---|---|---|---|---|---|---|
| sample | $\log(\bar{R}_h/\text{nm})$ | $\bar{X}_{de,n}$ | $\bar{X}_{de,w}$ | $\bar{X}_{de,n}$ | $\bar{X}_{de,w}$ | $\bar{X}_{de,n}$ | $\bar{X}_{de,w}$ | $T$ |
| parent rice starch | 1.35 | 16 | 18 | 76 | 93 | $7.2 \times 10^3$ | $1.4 \times 10^4$ | $3.0 \times 10^{-4}$ |
| F1 | 3.34 | 16 | 16 | 56 | 65 | | | |
| F2 | 3.04 | 14 | 16 | 62 | 87 | | | |
| F3 | 2.82 | 15 | 18 | 74 | 91 | | | |
| F4 | 2.56 | 16 | 18 | 68 | 88 | | | |
| F5 | 2.06 | 15 | 18 | 71 | 92 | $7.2 \times 10^3$ | $1.3 \times 10^4$ | $2.8 \times 10^{-4}$ |
| F6 | 1.65 | 15 | 19 | 74 | 96 | $7.5 \times 10^3$ | $1.2 \times 10^4$ | $3.3 \times 10^{-4}$ |
| F7 | 1.17 | 15 | 18 | 75 | 93 | $6.7 \times 10^3$ | $1.0 \times 10^4$ | $3.6 \times 10^{-4}$ |
| F8 | 1.10 | 15 | 19 | 82 | 88 | $5.0 \times 10^3$ | $9.3 \times 10^3$ | $3.7 \times 10^{-4}$ |
| F9 | 0.89 | 15 | 19 | 73 | 88 | $3.2 \times 10^3$ | $5.7 \times 10^3$ | $5.3 \times 10^{-4}$ |
| F10 | 0.67 | 15 | 19 | 78 | 92 | $1.4 \times 10^3$ | $2.5 \times 10^3$ | $1.6 \times 10^{-3}$ |

[a] Average size, number-average and weight-average degrees of polymerization $\bar{X}_{de,n}$ and $\bar{X}_{de,w}$, respectively. The rate ratio $T$ for the amylose component is also shown.

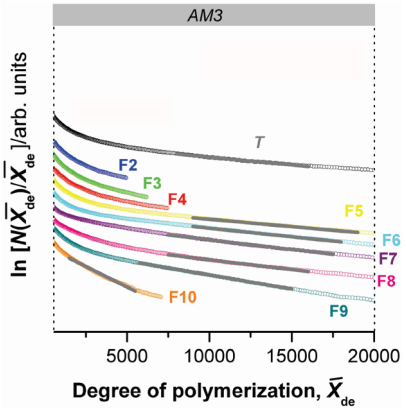


**Figure 6.** Kinetic plots, $\ln(N(\bar{X}_{de})/\bar{X}_{de})$, as a function of $\bar{X}_{de}$ for the debranched distributions for the amylose component. Points: experiment; lines: linear fitting to eq 5 for the amylose region.

suggests that

$$N(\bar{X}_{de}) \propto \bar{X}_{de} \exp(-T\bar{X}_{de}); \quad T = \frac{a_{SBE} + a_{DBE}}{a_{SS}} \qquad (5)$$

where $a_{SBE}$, $a_{DBE}$, and $a_{SS}$ are respectively the rates of actions of starch branching enzyme, starch debranching enzyme, and starch synthase, averaged across all isoforms. This treatment did not however take account of the fact that starch branching enzymes only operate on branches of DP greater than some minimum value, ~7 (e.g., ref 32). Equation 5 should be quantitatively applicable to amylose chains, where the branches are sufficiently long that the minimum-DP effect for branching enzyme is unimportant but is only semiquantitatively applicable to amylopectin branches. A treatment to take the minimum-DP effect into account has recently been developed.[33] However, this more precise treatment cannot be applied in the present case because the use of SEC for the branch-length distribution, necessary for technical reasons, means that the branch-length distribution for the amylopectin chains suffers significantly from band broadening,[14] which vitiates the accurate application of the more advanced treatment to the present data.

Being valid for amylose, eq 5 is used here to give a semiquantitative estimate of the ratio of chain stoppage to chain growth rates for the branch-length distributions at different sizes for this component. Equation 5 implies that a plot of $\ln([N(\bar{X}_{de})]/\bar{X}_{de})$ against $\bar{X}_{de}$ should be linear, with slope given by the rate ratio $T$. The value of $T$ is directly related to the average chain length (a large $T$ corresponding to a small $\bar{X}_{de}$). Figure 6 displays these kinetic plots for the rice starch and the corresponding fractions for the amylose component (AM3); the values for the rate ratio $T$ are displayed in Table 2 for each sample fraction and zone. The values of $T$ increase progressively with decreasing macromolecular size, as do the average DPs. This indicates different biosynthetic behavior for amylopectin and amylose architectures.

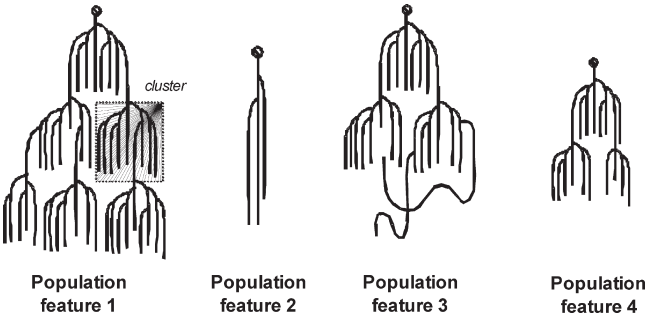


**Figure 7.** Sketch of the macromolecular architectures of the features found in native rice starch.

## Discussion

The 2-dimensional experimental studies reveal novel mechanistic information for the distinct macromolecular populations present in native rice starch. Four distinct features (two "mountains" and two "foothills") are seen in the 2-dimensional structural distribution plots (Figure 5). Feature 1 (a "mountain") corresponds to populations with large macromolecular sizes and short branches ($\bar{X}_{de} \sim 5-125$): amylopectin molecules. Feature 2 (the other "mountain") comprises amylose molecules with intermediate macromolecular sizes and larger branches ($\bar{X}_{de} \sim 400-20\,000$). A smaller "foothill", feature 3, is composed of large macromolecular sizes (about the same size as that of the main peak of amylopectin, $\bar{R}_h \sim 10^3$ nm) and medium branch lengths ($\bar{X}_{de} \sim 1000$) similar to amylose branches: like amylopectin with long-chain branches. Finally, a small "foothill", feature 4, is observed in the region of small macromolecular sizes ($\bar{R}_h \sim 10$ nm), with branch chain lengths corresponding to typical short amylopectin branches. This fourth feature could either be an intermediate component with amylopectin branching structure but with macromolecular sizes similar to amylose or an artifact from the fractionation during preparative SEC. It is significant that these smaller "foothills" (features 3 and 4), while apparent in the 2D distribution, cannot be distinguished in the parent 1D distribution (i.e., of the unfractionated starch, black lines in Figure 1). Sketches of the proposed macromolecular architectures of starch molecules in these features are presented in Figure 7.

The most important observations in these 2D distributions come from the main two features: the amylopectin and amylose "mountains". It is seen from feature 1, the amylopectin "mountain", that the debranched chain-length distributions for the short chains of amylopectin are similar for all the fractions; reflecting this, the average degrees of polymerization $\bar{X}_{de,n}$ and $\bar{X}_{de,w}$ show no systematic variation for the different fractions (Table 2). That is, the experimental 2D distribution function in this region is separable in $X_{de}$ and $V_h$. Hence, this part of the 2D distribution can be expressed (within experimental uncertainty) as the product of two separate functions: $w(\log V_h, X_{de}) = A(V_h)\, B(X_{de})$. Could this apparent separability be an artifact from the shear scission which, as stated, cannot be avoided for the large amylopectin whole molecules? While the size-separated fractions suffer some shear scission in this region, shear scission in SEC predominantly results in two large fragments, rather than one very large and one very small.[18] It would be a remarkable coincidence if this limited scission were to convert a nonseparable parent distribution into a separable one: chain scission is limited to a small number of linkages throughout the whole branched structure and should not affect the overall branch chain distribution. It is therefore reasonable to suppose that the parent (unbroken) distribution is also separable, i.e., that in the amylopectin region, the branch-length distribution is independent of total molecular size.

The 2D data thus imply that the branching structure of amylopectin is completely independent of the size of the whole molecule: the branching architecture of amylopectin is the same throughout all scales of macromolecular size. This conclusion is in fact a very reasonable one. The biological function of starch in starch-accumulating plants, such as the rice used here, is energy storage for the germinating seed. The "right" energy storage comes from the crystalline structure of the alternating lamellae, formed by α-helices between pairs of short branches of amylopectin within a cluster (Figure 7, population feature 1).[34] The formation of a crystalline lamella is highly likely only to be possible within a fairly narrow range of branch distributions because the branch distributions seen in starch-synthesizing plants are all semiquantitatively similar (e.g., ref 31). Any mutations in a plant that results in a significantly different branch distribution would therefore be discriminated against in evolution and thus would not be seen in native (or cultivated) plants. The observation of an amylopectin branch distribution that is independent of whole-molecule size reinforces these inferences: the biological imperative of a tightly constrained range of branch-length distributions of short branches, linked within a cluster, which are able to form crystalline lamellae.

Feature 2, the amylose "mountain", shows that amylose macromolecular architectures, in contrast to those of amylopectin, exhibit a systematic variation of branched-chain-length distributions with total macromolecular size. Reflecting this, the average branch length $\bar{X}_{de}$ increases (and the rate ratio $T$ decreases) with increasing hydrodynamic volume (Table 2). Thus, the mechanism controlling amylose formation must include a whole-molecule size-dependent term. Amylose biosynthesis has often been described as a downstream process from that of amylopectin and involves a different propagation enzyme (GBSS, granule-bound starch synthase, rather than, or in addition to, starch synthase).[11,35,36] The mechanisms that completely terminate the growth of an entire starch molecule (as distinct from those that cause a single branch to terminate), and thus determine total molecular size ($V_h$), are not well understood and may well be under the control of total size itself (crowdedness) and/or under diurnal control. However, it is accepted that GBSS is located in confined regions within the granule matrix.[37] Thus, it is not unreasonable to suppose that the branch termination process for amylose molecules may be influenced by total molecular size.

The presence of long-chain branches in amylopectin-like architectures (feature 3) has been reported by other authors as "extra-long" or "super-long" chains.[38−40] This hybrid component could not simply be molecules containing long amylopectin branches which span three crystalline lamellae: branches spanning three lamellae have maxima at DP ∼ 70,[41] which is outside the region where the intermediate foothill is found. The possibility of elution of amylose-type macromolecules (feature 2) in such fractions due to band broadening during SEC fractionation can be discarded because if that were the case, the debranched distributions would rather exhibit larger branches with $\bar{X}_{de} \sim 7000$, similar to the debranched distributions of fractions F5 and F6, rather than the smaller observed values of $\bar{X}_{de} \sim 1000$. The existence of these long-chain amylopectin-like architectures manifest in feature 3 can be explained from the mechanism of amylose biosynthesis by GBSS using amylopectin short branches as primers for elongation[11] and has been experimentally demonstrated by the introduction of a rice *Wx* gene encoding GBSS into a waxy rice.[40] Recent theory[33] also shows that mutations leading to such intermediates would not be discriminated against by evolutionary pressure. The appearance of a small peak corresponding to long chain branches of $\bar{X}_{de} \sim 1000$ for the fractions with higher macromolecular sizes (F2−F4) can only be ascribed to the presence of such hybrid macromolecular architectures.

Amylopectin-like short-chain branches are found in the debranched distributions for all the preparative SEC fractions, principally for higher macromolecular sizes, feature 1 (amylopectin), but also in smaller quantities in the fractions corresponding to smaller macromolecular sizes (feature 4). Thus amylopectin-like populations may have a wide range of sizes in rice starch, from $\bar{R}_h \sim 10$ to 3000 nm. There are some hints of this small-amylopectin effect in literature data, which has been identified as an intermediate component with amylopectin-like branching structure but with macromolecular sizes similar to amylose.[42,43] In the Supporting Information, it is shown that this feature is unlikely to be an experimental artifact. Being able to observe the presence of small amylopectin molecules in the present system, where there is also a significant fraction of amylose present, is only possible by the 2D technique developed here; the small-amylopectin component is masked by the amylose component in 1D distributions. If (as we believe) the observation of significant amounts of small amylopectin molecules is not an artifact, then it would be expected also to be apparent in pure amylopectin samples, i.e., for a native waxy starch. At present, there seem to be no data in the literature for size distributions of waxy (100% amylopectin) native starch obtained under conditions[19] such there was no degradation of the starch during the extraction and dissolution process (although there are data for commercially extracted starch[20] which may have suffered degradation). The implications of the observation that there are probably very small amylopectin molecules are not yet apparent; if this observation is indeed found to be artifact-free, then it needs to be taken into account in descriptions of starch biosynthesis, for which there are significant unresolved questions.[22,37,44,45]

Interpretation of the 2D number distributions is difficult at this point. It is important to realize that while size and number distributions are trivially related for linear polymer, eq 4, there is no such relation for branched polymers: the number and weight distributions include complementary information. Number distributions are controlled by the various mechanisms initiating whole starch molecules, adding monomer units, and completely terminating the growth of the whole molecule; as stated, this last mechanism is not known at this point. In the future, data obtained using the technique given here should shed light on the nature of this process.

The number distributions of the branched and debranched fractions (Figure 3) tend to superpose in the amylose region for

the fractions with smaller macromolecular sizes. This is as expected. There are relatively few branches in amylose, and thus smaller amylose molecules contain fewer branches; in the limit of no branches, which will also be the small-molecule limit, then the branched and debranched size distributions will trivially be the same.

## Conclusions

This paper reports the first two-dimensional structural distribution for a branched polymer in which the separation parameters are well-defined: the hydrodynamic volume and the branch length. Such distributions have the potential to reveal new information about synthesis mechanisms and about structure−property relations. The 2D distributions were obtained first using fractionation by preparative size exclusion chromatography and subsequent enzymatic debranching of these fractions; both whole and debranched samples were analyzed using analytical SEC and multiple detection to obtain their size and branch chain-length distributions. The two-dimensional distributions for native rice starch obtained here reveal hitherto unreported structural features of the macromolecular populations present. These distributions show four distinct features: a "mountain" of molecules with large size and many small branches, which is amylopectin; another "mountain" with smaller size and longer branches, which is amylose; a "foothill" which is best thought of as a hybrid component of relatively large (amylopectin-like) molecules but with a significant number of long-chain branches; and a last "foothill" corresponding to molecules with typical amylopectin branching structure but with macromolecular sizes similar to amylose. This observation, if it is artifact-free, reinforces other data in the literature, suggesting the presence of an intermediate starch.

The 2D distribution show that amylopectin molecules have a branching structure that is independent of macromolecular size. On the other hand, amylose molecules exhibit a systematic variation in branching structure with increasing macromolecular size. These structural differences can be interpreted from, and shed light on, current understanding of the biosynthetic pathways during starch biosynthesis. Amylopectin biosynthesis is restricted by evolutionary pressure to yield a well-defined branching structure for all scales of macromolecular sizes so as to give an efficient energy storage molecule for the germinating plant: being able to arrange in the hierarchical cluster structure independently of overall macromolecular size. Mutations in a plant which do not give such a structure will place the plant at an evolutionary disadvantage and so will not last a generation or two. Amylose biosynthesis is not restricted by such constraints, offering a wide range of branching architectures. Indeed, the branch distribution in amylose is controlled by some process which this study reveals to depend on molecular size; this is an area of future investigation. This has significant implications for nutrition, since starches containing longer chains tend to have beneficial digestion properties in humans.[46,47] The 2D distributions which can be obtained using the method given in the present paper have the potential to shed light upon the processes controlling these chain lengths and on the mechanism(s) which terminate overall growth of the whole molecule.

The methodology developed here can be applied to any branched biological or synthetic homopolymer which can be quantitatively debranched.

**Acknowledgment.** R.G.G. gratefully acknowledges the support of an Australian Research Council grant (DP0986043), and F.V. greatly appreciates the support of a postdoctoral fellowship from the Knut and Alice Wallenberg Foundation (Sweden). Constructive discussions with Prof. Mike Gidley, Dr. Jovin Hasjim, and Alex Chi Wu are also greatly appreciated.

**Supporting Information Available:** Details of preparative SEC; details of calibration; possible artifacts. This material is available free of charge via the Internet at http://pubs.acs.org.

## References and Notes

(1) Jones, R. G.; Kahovec, J.; Stepto, R.; Wilks, E. S.; Hess, M.; Kitayama, T.; Metanomski, W. V. *Compendium of Polymer Terminology and Nomenclature. IUPAC Recommendations 2008*; Royal Society of Chemistry: Cambridge, 2009.
(2) Gray-Weale, A.; Gilbert, R. G. *J. Polym. Sci., Part A: Polym. Chem. Ed.* **2009**, *47*, 3914–3930.
(3) Kilz, P.; Kruger, R. P.; Much, H.; Schulz, G. *Adv. Chem. Ser.* **1995**, *247*, 223–241.
(4) Adrian, J.; Esser, E.; Hellmann, G.; Pasch, H. *Polymer* **2000**, *41*, 2439–2449.
(5) van der Horst, A.; Schoenmakers, P. J. *J. Chromatogr., A* **2003**, *1000*, 693–709.
(6) Edam, R.; Meunier, D. M.; Mes, E. P. C.; Van Damme, F. A.; Schoenmakers, P. J. *J. Chromatogr., A* **2008**, *1201*, 208–214.
(7) Meunier, D. M.; Smith, P. B.; Baker, S. A. *Macromolecules* **2005**, *38*, 5313–5320.
(8) Khalyavina, A.; Schallausky, F.; Komber, H.; Al Samman, M.; Radke, W.; Lederer, A. *Macromolecules* **2010**, *43*, 3268–3276.
(9) Rosselgong, J.; Armes, S. P.; Barton, W. R. S.; Price, D. *Macromolecules* **2010**, *43*, 2145–2156.
(10) Libessart, N.; Maddelein, M. L.; Vandenkoornhuyse, N.; Decq, A.; Delrue, B.; Mouille, G.; Dhulst, C.; Ball, S. *Plant Cell* **1995**, *7*, 1117–1127.
(11) van de Wal, M.; D'Hulst, C.; Vincken, J. P.; Buleon, A.; Visser, R.; Ball, S. *J. Biol. Chem.* **1998**, *273*, 22232–22240.
(12) Tziotis, A.; Seetharaman, K.; Wong, K. S.; Klucinec, J. D.; Jane, J. L.; White, P. J. *Cereal Chem.* **2004**, *81*, 611–620.
(13) Schmitz, S.; Dona, A. C.; Castignolles, P.; Gilbert, R. G.; Gaborieau, M. *Macromol. Biosci.* **2009**, *9*, 506–514.
(14) Castro, J. V.; Ward, R. M.; Gilbert, R. G.; Fitzgerald, M. A. *Biomacromolecules* **2005**, *6*, 2260–2270.
(15) Morell, M. K.; Samuel, M. S.; O'Shea, M. G. *Electrophoresis* **1998**, *19*, 2603–2611.
(16) O'Shea, M. G.; Samuel, M. S.; Konik, C. M.; Morell, M. K. *Carbohydr. Res.* **1998**, *307*, 1–12.
(17) Gaborieau, M.; Gilbert, R. G.; Gray-Weale, A.; Hernandez, J. M.; Castignolles, P. *Macromol. Theory Simul.* **2007**, *16*, 13–28.
(18) Cave, R. A.; Seabrook, S. A.; Gidley, M. J.; Gilbert, R. G. *Biomacromolecules* **2009**, *10*, 2245–2253.
(19) Gidley, M. J.; Hanashiro, I.; Hani, N. M.; Hill, S. E.; Huber, A.; Jane, J.-L.; Liu, Q.; Morris, G. A.; Rolland-Sabaté, A.; Striegel, A.; Gilbert, R. G. *Carbohydr. Polym.* **2010**, *79*, 255–261.
(20) Rolland-Sabate, A.; Colonna, P.; Mendez-Montealvo, M. G.; Planchot, V. *Biomacromolecules* **2007**, *8*, 2520–2532.
(21) Syahariza, Z. A.; Li, E.; Hasjim, J. *Carbohydr. Polym.* **2010**, in press (DOI: 10.1016/j.carbpol.2010.1004.1014).
(22) Vandeputte, G. E.; Delcour, J. A. *Carbohydr. Polym.* **2004**, *58*, 245–266.
(23) Shortt, D. W. *J. Liq. Chromatogr.* **1993**, *16*, 3371–3391.
(24) Clay, P. A.; Gilbert, R. G. *Macromolecules* **1995**, *28*, 552–569.
(25) Nakamura, Y.; Sakurai, A.; Inaba, Y.; Kimura, K.; Iwasawa, N.; Nagamine, T. *Starch/Staerke* **2002**, *54*, 117–131.
(26) Hizukuri, S. *Carbohydr. Res.* **1985**, *141*, 295–306.
(27) Jane, J.; Chen, Y. Y.; Lee, L. F.; McPherson, A. E.; Wong, K. S.; Radosavljevic, M.; Kasemsuwan, T. *Cereal Chem.* **1999**, *76*, 629–637.
(28) Takeda, Y.; Hizukuri, S.; Juliano, B. O. *Carbohydr. Res.* **1989**, *186*, 163–166.
(29) Hanashiro, I.; Takeda, Y. *Carbohydr. Res.* **1998**, *306*, 421–426.
(30) Chen, M.-H.; Bergman, C. J. *Carbohydr. Polym.* **2007**, *69*, 562–578.
(31) Castro, J. V.; Dumas, C.; Chiou, H.; Fitzgerald, M. A.; Gilbert, R. G. *Biomacromolecules* **2005**, *6*, 2248–2259.
(32) Guan, H.; Li, P.; Imparl-Radosevich, J.; Preiss, J.; Keeling, P. *Arch. Biochem. Biophys.* **1997**, *342*, 92–98.
(33) Wu, A. C.; Gilbert, R. G., submitted.
(34) Fitzgerald, M. A. In *Rice Chemistry and Technology*; Champagne, E. T., Ed.; AACC: St Paul, MN, 2004.
(35) Denyer, K.; Johnson, P.; Zeeman, S. C.; Smith, A. M. *J. Plant Physiol.* **2001**, *158*, 479–487.

(36) Ball, S. G.; van de Wal, M. H. B. J.; Visser, R. G. F. *Trends Plant Sci*. **1998**, *3*, 462–467.
(37) Ball, S. G.; Morell, M. K. *Annu. Rev. Plant Biol*. **2003**, *54*, 207–233.
(38) Takeda, Y.; Hizukuri, S. *Carbohydr. Res*. **1987**, *168*, 79–88.
(39) Takeda, Y.; Maruta, N.; Hizukuri, S. *Carbohydr. Res*. **1989**, *187*, 287–294.
(40) Hanashiro, I.; Itoh, K.; Kuratomi, Y.; Yamazaki, M.; Igarashi, T.; Matsugasako, J.-i.; Takeda, Y. *Plant Cell Physiol*. **2008**, *49*, 925–933.
(41) Bultosa, G.; Hamaker, B. R.; BeMiller, J. N. *Starch-Staerke* **2008**, *60*, 8–22.
(42) Zhong, F.; Yokoyama, W.; Wang, Q.; Shoemaker, C. F. *J. Agric. Food Chem*. **2006**, *54*, 2320–2326.
(43) Yoo, S.-H.; Jane, J.-L. *Carbohydr. Polym*. **2002**, *49*, 307–314.
(44) Hannah, L. C.; James, M. *Curr. Opin. Biotechnol*. **2008**, *19*, 160–165.
(45) Robyt, J. F. *Biologia* **2008**, *63*, 980–988.
(46) Bird, A. R.; Vuaran, M. S.; King, R. A.; Noakes, M.; Keogh, J.; Morell, M. K.; Topping, D. L. *Br. J. Nutr*. **2008**, *99*, 1032–1040.
(47) Regina, A.; Bird, A.; Topping, D.; Bowden, S.; Freeman, J.; Barsby, T.; Kosar-Hashemi, B.; Li, Z.; Rahman, S.; Morell, M. *Proc. Natl. Acad. Sci. U.S.A*. **2006**, *103*, 3546–3551.